Low-voltage-driven pentacene thin-film transistor with an organic-inorganic nanohybrid dielectric

Kwang H. Lee, Jeong-M. Choi, and Seongil ImByoung H. Lee, Kyo K. Im, and Myung M. SungSeungjun Lee

Citation: Appl. Phys. Lett. **91**, 123502 (2007); doi: 10.1063/1.2786595
View online: http://dx.doi.org/10.1063/1.2786595
View Table of Contents: http://aip.scitation.org/toc/apl/91/12
Published by the American Institute of Physics

Low-voltage-driven pentacene thin-film transistor with an organic-inorganic nanohybrid dielectric

Kwang H. Lee, Jeong-M. Choi, and Seongil Im[a)]
Institute of Physics and Applied Physics, Yonsei University, Seoul 120-749, Korea

Byoung H. Lee, Kyo K. Im, and Myung M. Sung
Department of Chemistry, Hanyang University, Seoul 133-791, Korea

Seungjun Lee
Information Electronics Engineering, Ewha Womans University, Seoul 120-750, Korea

(Received 20 July 2007; accepted 29 August 2007; published online 18 September 2007)

The authors report on the fabrication of pentacene-based thin-film transistors (TFTs) with a 13 nm-thick nanohybrid superlattice-type dielectric composed of ten units of molecular aluminum oxide (AlO_x)-self-assembled multilayer (SAMu) lattice on indium-tin-oxide (ITO) glass or on n^+-Si substrate. The AlO_x-SAMu nanohybrid layers showed high dielectric capacitances of 187 and 233 nF/cm^2 on ITO glass and on n^+-Si substrate, respectively, along with a high dielectric strength of 4 MV/cm in both cases. Our pentacene-TFTs showed a maximum field effect mobility of 0.92 cm^2/V s, operating at −3 V with an on/off current ratio of $\sim 10^3$. Load-resistance inverter using our pentacene-TFT demonstrated a decent voltage gain of ~5. © *2007 American Institute of Physics*. [DOI: 10.1063/1.2786595]

Organic thin-film transistors (OTFTs) have been extensively studied over the past few decades due to their potentials toward low-cost, simple, and low-temperature processes based on glass or plastics.[1–3] Especially, pentacene-based OTFTs have been extensively studied because of their high field mobility of over 0.5 cm^2/V s.[1–3] Recently, low-driven voltage pentacene-TFTs have also been reported with various gate dielectric layers: thin polymers,[4,5] self-assembled monolayer (SAM),[6] high-k metal oxide,[7,8] and thin polymer/thick high-k oxide double layer.[9] In all the cases of dielectrics the first important issue was how to keep their own high dielectric capacitances without any serious gate current leakage and the second issue was how to achieve an optimally hydrophobic smooth surface for good crystalline growth of solid pentacene. One way to satisfy the above two important issues was adopting both organic thin hydrophobic layer and inorganic high-k dielectric layer in stack,[9] although the organic-inorganic hybrid double layer approach could be disadvantageous in that it should go through two different processes: physical vapor deposition and spin casting. In the present study, we thus suggest another solution that takes after the organic-inorganic hybrid dielectric approach but uses only one simple process step, the so-called organic-inorganic nanohybrid technique.

Both substrates of indium tin oxide (ITO)/glass and heavily doped silicon (n^+-Si) were cleaned with acetone, methanol, and de-ionized water, in that order. Ten units of molecular aluminum oxide (AlO_x)-self-assembled multilayer (SAMu) lattice were deposited on ITO and on n^+-Si substrates by molecular layer deposition (MLD) which is similar to atomic layer deposition (ALD) in the aspect of using gas phase reaction. One unit of AlO_x-SAMu lattice is 1.3 nm thin in theoretical approximation, as shown in the right-side inset of Fig. 1(a). Our MLD process was conducted by repeating the following three steps: adsorption of 7-octadecyltrichlorosilane (OTS), ozone-induced modification of 7-OTS (to be ended with COOH, carboxylic group), and activation of carboxylated 7-OTS to chemically adsorb aluminum hydroxyl groups. Alkene-terminated self-assembled monolayers were formed by flowing the $[CH_2{=}CH(CH_2)_6SiCl_3]$ (Aldrich: 96%) and H_2O vapor onto clean Si substrate at the temperature of 200 °C in the MLD chamber. The terminal C=C groups of the SAMu were converted to carboxylic acid groups by ozone treatment in the same chamber, providing active adsorption sites for the formation of AlO_x-SAMu. The aluminum hydroxyl were then deposited on the COOH-terminated SAMu by using $[Al(OCH(CH_3)_2)_3]$ (Aldrich: 99.999%) and H_2O as usual ALD precursors [Fig. 1(a) shows one unit of AlO_x-SAMu lattice]. Ten cycles of the unit inorganic-organic (AlO_x-SAMu) lattice formation were taken under a pressure of 300 mtorr, so that the total thickness of the nanohybrid AlO_x-SAMu dielectric layer might be around 13 nm. (The total thickness was confirmed by high resolution transmission electron microscopy as we inserted the nanohybrid dielectric layer between two thin AlO_x layers for a resolvable thickness image with good contrast [see Fig. 1(b).] The top surface of the nanohybrid AlO_x-SAMu dielectric was finished without ozone treatment, so that the final dielectric surface is quite hydrophobic as evaluated by contact angle measurement (contact angle was ~90°). Pentacene (Aldrich Chem. Co., 99% purity, no other distillation) active channel layer was patterned on the AlO_x-SAMu dielectric through a shadow mask at room temperature (RT) by thermal evaporation. Deposition rate was fixed to 1 Å/s using an effusion cell (ALPHAPLUS Co., LTE-500S) in a vacuum chamber (base pressure of $\sim 1\times 10^{-7}$ torr). The thickness of pentacene films was 50 nm as monitored by a quartz crystal oscillator and confirmed by ellipsometry. Au pads were finally deposited as source and drain electrodes by thermal evaporation in a vacuum chamber (base pressure of ~2

[a)]Author to whom correspondence should be addressed. Tel.: 82-2-2123-2842. FAX: 82-2-392-1592. Electronic mail: semicon@yonsei.ac.kr

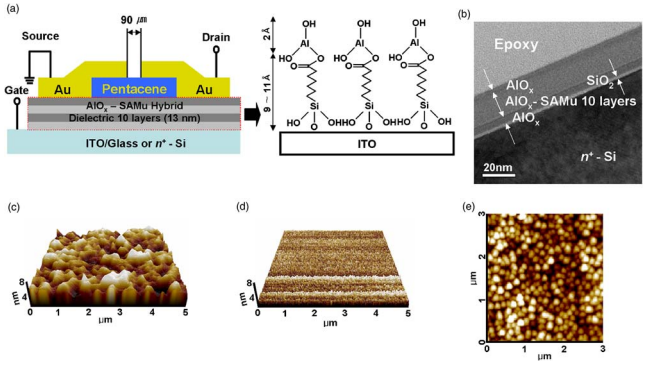

FIG. 1. (Color online) (a) Schematic cross section of our pentacene-TFT with 13-nm-thick AlO_x-SAMu nanohybrid insulator. Right-side inset: the scale of one unit AlO_x-SAMu. (b) High resolution TEM image of our nanohybrid insulator inserted between two thin AlO_x films. Here we used n^+-Si with 2-nm-thin native oxide as a substrate for TEM samples. AFM images of the 13-nm-thick AlO_x-SAMu (c) on ITO glass and (d) on n^+-Si substrates (5×5 μm^2). (e) AFM surface image of pentacene channel grown on nanohybrid dielectric layer (3×3 μm^2).

$\times10^{-6}$ torr). As shown in the schematic cross-sectional view of Fig. 1(a), the nominal channel (L) and width (W) of our pentacene-TFTs were 90 and 500 μm, respectively.

The electrical properties of the AlO_x-SAMu dielectric films were measured with 300 μm diameter Au dot/dielectric/ITO and the Au dot/dielectric/n^+-Si structures by capacitance-voltage (C-V) and current density-electric field (J-E) tests. The dielectric and pentacene surface morphologies were observed by atomic force microscopy (AFM) (XE-100, PSIA).

Figures 1(c) and 1(d) show the AFM surface images of the 13-nm-thin (nanohybrid) AlO_x-SAMu dielectric films on ITO glass and on n^+-Si substrates, respectively. According to Figs. 1(c) and 1(d), the surface roughness values of AlO_x-SAMu films on ITO glass and on n^+-Si substrate were 1.0 and 0.2 nm, respectively. Those roughness values are almost the same as those of ITO and n^+-Si since the surface contour of our thin dielectric directly follows that of its substrate as a result of layer-by-layer growth by molecular gas reaction.[10] Figure 1(e) is the surface morphology of pentacene channel grown on the nanohybrid dielectric, whose surface is quite hydrophobic, finished with SAMu layer. Almost the same pentacene surface image was obtained regardless of whether the growth substrate was the nanohybrid layer on ITO or on n^+-Si, and the surface image is comparable to that obtained after growth on typical hydrophobic SAMs such as OTS.[11,12] According to previous reports, the pentacene channel formed on OTS has a good channel/dielectric interface, resulting in a relatively good field mobility although the surface morphology is not dendritic.[12,13]

Figure 2 shows C-V and J-E characteristics of the 13-nm-thin AlO_x-SAMu dielectrics on n^+-Si and on ITO. The dielectric constants (k) of the nanohybrid dielectric layer on ITO glass and on n^+-Si substrate were ~2.74 and ~3.43, respectively, estimated from the measured capacitance values (on ITO: 187 nF/cm^2 and on n^+-Si: ~233 nF/cm^2). The reason why the dielectric capacitance of the nanohybrid dielectric on ITO appears lower than that on ITO glass might be attributed to its inferior interface roughness, as observed in Fig. 1(c). The rough interface between electrode and dielectric easily causes leakage current and also results in reduced dielectric capacitance because deposited metal electrode may

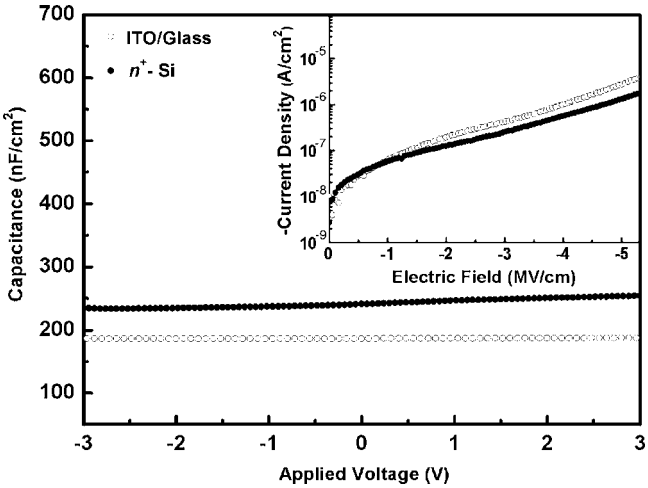

FIG. 2. Capacitance-voltage (C-V) curves of AlO_x-SAMu (13 nm) dielectric insulators on ITO glass and n^+-Si substrate as measured from 300 μm-diameter Au dot /dielectric/electrode structures. The inset shows current density-electric field (J-E) characteristics of the nanohybrid insulators.

not perfectly cover the rough dielectric surface.[14] As an evidence shown in the J-E curve of Fig. 2 (inset), the nanohybrid dielectric film on smooth n^+-Si substrate appeared to have a slightly better dielectric strength (~4.0 MV/cm in our maximum leakage current standard of ~10^6 A/cm^2) and better leakage current behavior than the dielectric on ITO, which has relatively rough surface. By the way, it is also

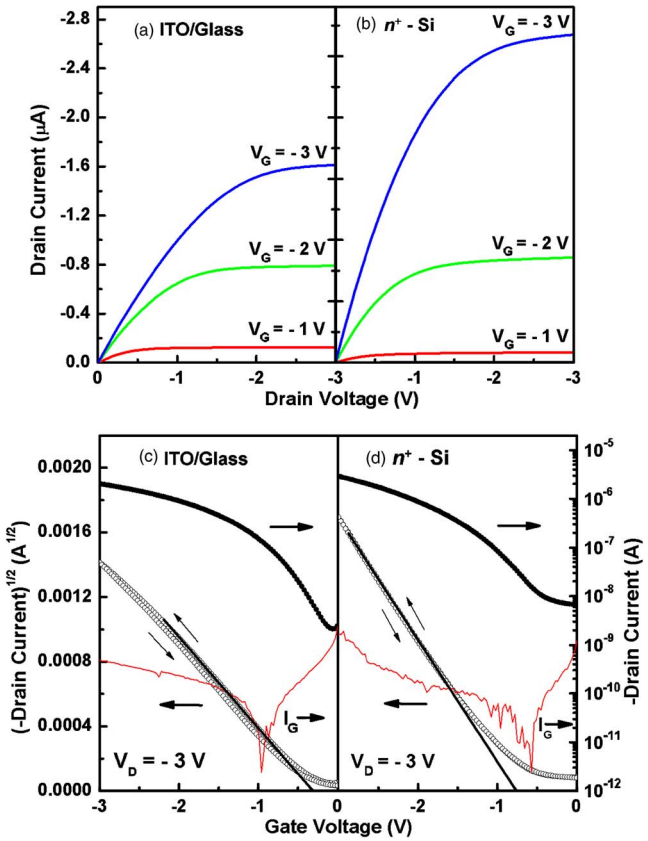

FIG. 3. (Color online) Drain current-drain voltage (I_D-V_D) output curves obtained from our pentacene-TFTs with the nanohybrid dielectrics prepared on (a) ITO glass and (b) on n^+-Si substrates. Transfer curves [$\sqrt{-I_D}$-V_G and $\log_{10}(-I_D)$-V_G] of the pentacene-TFTs prepared on (c) ITO and on (d) n^+-Si substrates (V_D=−3 V).

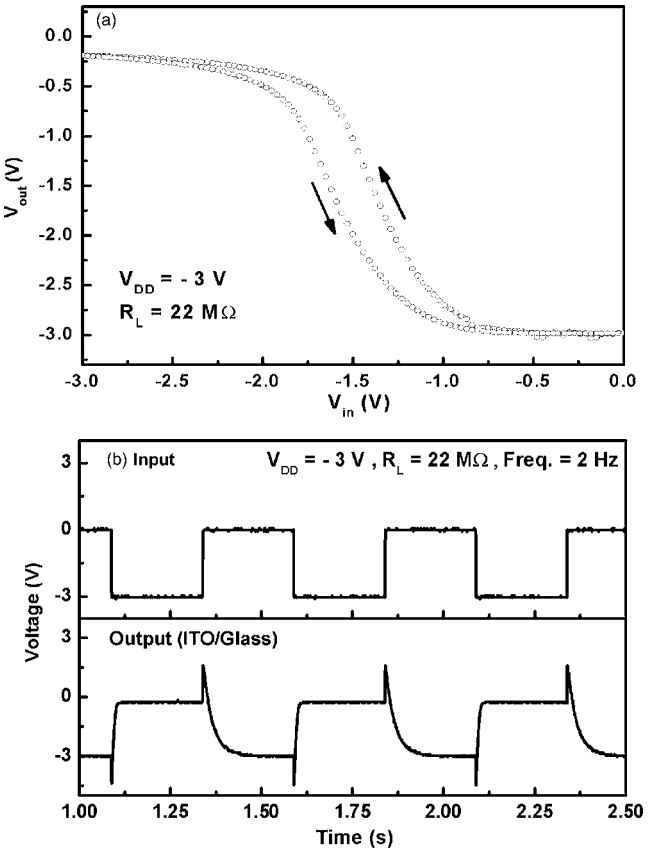

FIG. 4. Properties of our resistance-load inverter. Our inverter was composed of a pentacene-TFT (with the 13-nm-thick nanohybrid dielectric on ITO glass) and a load resistor R_L=22 MΩ. (a) Static behavior of our resistance-load inverter. (b) Dynamic behavior of the same inverter. Input voltage signal by pulse generator (2 Hz) and output voltage signal (V_{DD}=−3 V).

worthy of note that despite such thin layer thickness of 13 nm our nanohybrid layer sustains the large electric field of 4 MV/cm without much current leakage, resulting in a very high capacitance over ~187 nF/cm^2.

Figures 3(a) and 3(b) exhibit the drain current-drain voltage (I_D-V_D) output curves obtained from our pentacene-based TFTs with the 13-nm-thin nanohybrid dielectric layers on the two different substrates: ITO glass and n^+-Si. All devices operated at lower than −3 V. Maximum saturation current of ~2.8 μA was achieved under a gate bias of −3 V from the OTFT prepared on n^+-Si, while about 1.6 μA was observed from the other one on ITO glass, in which case the dielectric showed a lower capacitance (Fig. 2) and inferior surface roughness [Fig. 1(c)]. According to the drain current-gate voltage (I_D-V_G) transfer curves of Figs. 3(c) and 3(d), the pentacene-TFT prepared on n^+-Si showed two times higher field mobility (saturation regime mobility) of 0.92 cm^2/V s than that of the other one on ITO glass substrate (0.47 cm^2/V s). This result on the mobility difference is probably attributed to the channel/dielectric interface roughness [see Figs. 1(c) and 1(d)]. The threshold voltages (V_T) of pentacene-TFTs were about −0.75 V on n^+-Si substrate and −0.3 V on ITO glass, but both TFT devices showed only a little amount of gate-bias hysteresis, evidencing that the present nanohybrid dielectric possesses quite a good gate stability. Although the $\log_{10}(-I_D)-V_G$ curves of Figs. 3(c) and 3(d) showed an on/off current ratio of less than ~10^3 for both devices, it is notable that the maximum gate leakage current (I_G) level is kept under less than 1 nA in spite of the 10-nm-scale dielectric thickness.

Figure 4(a) exhibits voltage transfer characteristics (VTCs) of a load-resistance inverter which consists of a pentacene-TFT (on ITO glass) and 22 MΩ load while Fig. 4(b) shows its dynamic inverting behavior.[15,16] According to the VTC curves of Fig. 4(a), our inverter operates well at a low supplied voltage (V_{DD}) of 3 V, demonstrating a decent output voltage gain ($\partial V_{out}/\partial V_{in}$) of ~5. The inverter hysteresis seems to stem from the small I_D-V_G hysteresis observed in Fig. 3(c). Its dynamic inverter action was clearly observed during input (gate) biasing with a square wave [frequency of 2 Hz, see Fig. 4(b)], but it does not really make squarelike output waves due to a high overlap capacitance in the TFT device structure,[17] which produces large on- and off-delay times (*RC* delays) of 1.0 and 50 ms, respectively, along with boost-up effect peaks. The static and dynamic inverting behavior, however, again supports the fact that our thin organic-inorganic nanohybrid dielectric plays well as a gate insulator at a low voltage for pentacene-TFTs.

We thus conclude that our thin nanohybrid layer is quite a promising candidate as a gate dielectric for low-voltage driven pentacene-TFTs.

The authors acknowledge the financial support from KOSEF (Program No. Ml-0214-00-0228) and Brain Korea 21 Project.

[1] C. D. Sheraw, L. Zhou, J. R. Huang, D. J. Gundlach, T. N. Jackson, M. G. Kane, I. G. Hill, M. S. Hammond, J. Campi, B. K. Greening, J. Francl, and J. West, Appl. Phys. Lett. **80**, 1088 (2002).
[2] U. Zschieschang, H. Klauk, M. Halik, G. Schmid, and C. Dehm, Adv. Mater. (Weinheim, Ger.) **15**, 1147 (2003).
[3] H. Klauk, M. Halik, U. Zschieschang, F. Eder, G. Schmid, and C. Dehm, Appl. Phys. Lett. **82**, 4175 (2003).
[4] M. J. Panzer, C. R. Newman, and C. D. Frisbie, Appl. Phys. Lett. **86**, 103503 (2005).
[5] C. D. Dimitrakopoulos, S. Purushothaman, J. Kymissis, A. Callegari, and J. M. Shaw, Science **283**, 822 (1999).
[6] M. Halik, H. Klauk, U. Zschieschang, G. Schmid, C. Dehm, M. Schutz, S. Malsch, F. Effenberger, M. Brunnbauer, and F. Stellacci, Nature (London) **431**, 963 (2004).
[7] Y. Liang, G. Dong, Y. Hu, L. Wang, and Y. Qiu, Appl. Phys. Lett. **86**, 132101 (2005).
[8] K. D. Kim and C. K. Song, Appl. Phys. Lett. **88**, 233508 (2006).
[9] D. K. Hwang, C. S. Kim, J. M. Choi, K. Lee, J. H. Park, E. Kim, H. K. Baik, J. H. Kim, and S. Im, Adv. Mater. (Weinheim, Ger.) **18**, 2299 (2006).
[10] D. B. Mitzi, Chem. Mater. **13**, 3283 (2001).
[11] W. Kalb, P. Lang, M. Mottaghi, H. Aubin, G. Horowitz, and M. Wuttig, Synth. Met. **146**, 279 (2004).
[12] M. Shtein, J. Mapel, J. B. Benziger, and S. R. Forrest, Appl. Phys. Lett. **81**, 268 (2002).
[13] J. Lee, J. H. Kim, D. Y. Jung, and S. Im, J. Appl. Phys. **96**, 2301 (2004).
[14] Y.-P. Zhao, G.-C. Wang, T.-M. Lu, G. Palasantzas, and J. Th. M. De Hosson, Phys. Rev. B **60**, 9157 (1999).
[15] S. D. Vusser, S. Steudel, K. Myny, J. Genoe, and P. Heremans, Appl. Phys. Lett. **88**, 162116 (2006).
[16] H. Klauk, U. Zschieschang, J. Pflaum, and M. Halik, Nature (London) **445**, 745 (2007).
[17] M. Fadlallah, W. Benzarti, G. Billiot, W. Eccleston, and D. Barclay, J. Appl. Phys. **99**, 104504 (2006).